International Journal of Computational and Experimental Science and ENgineering (IJCESEN)

Vol. 10-No.4 (2024) pp. 983-987
http://www.ijcesen.com

ISSN: 2149-9144

Research Article

X-ray Investigation of the Supernova Remnant Candidate G278.0+12.4 and Prospect of Future Missions

Ebru AKTEKİN ÇALIŞKAN*

Süleyman Demirel University, Engineering and Natural Sciences Faculty, Physics Department, 32200, Isparta-Turkiye
* **Corresponding Author Email:** ebrucaliskan@sdu.edu.tr - **ORCID:** 0000-0002-5904-4580

Article Info:

DOI: 10.22399/ijcesen.547
Received : 22 October 2024
Accepted : 14 November 2024

Keywords:

Supernova Remnants
G278.0+12.4
X-rays
Simulations

Abstract:

In this work, we analyze the X-ray data of supernova remnant (SNR) candidate G278.0+12.4. We examine its nature and the X-ray properties such as electron temperature kTe and abundances, using Suzaku data. We found that the X-ray emission is well represented by two-component model: an absorbed thermal plasma with about 5 keV and non-thermal plasma with a photon index ~ 0.5-1. Our spectral analysis confirms that the G278.0+12.4 is likely to be an SNR. We found non-thermal X-ray emission from the spectra, which indicates that a pulsar wind nebula scenario is possible for G278.0+12.4. In order to make predictions for future missions, we perform XRISM and Athena simulations. We present our results on the nature of G278.0+12.4.

1. Introduction

The *ROSAT* All-Sky Survey conducted an all-sky survey in the X-ray energy range between 0.1 and 2.4 keV [1]. This X-ray survey identified numerous extended and point-like sources, many of which were previously unknown. The detected sources include objects such as supernova remnants (SNRs), pulsars, and binary stars.

Supernovae (SN) are among the most powerful (about 10^{51} erg) events in the Universe. The primary source of heavy element synthesis in galaxies is SN. This tremendous explosion sends gas (ejecta) into the interstellar medium (ISM), where it travels as a shock wave. The ejecta interacts with and incorporates the ISM, increasing its overall mass. The oncoming shock wave raises the temperature of the gas in front of it (about $10^6 - 10^7$ K). This gas generates thermal radiation with X-ray wavelengths. An essential tool for diagnosing ISM is X-ray measurements ([2], for a review). G278.0+12.4 is an SNR candidate detected by the *ROSAT* all-sky Survey [3]. With high-resolution X-ray spectral observations, it can be determined whether this object is an SNR. No comprehensive X-ray analysis of this source exists in the literature. As a result, the origin of the X-ray emission from G278.0+12.4 is still unclear, and its distance is also uncertain.

In this work, we investigate the X-ray spectral properties of G278.0+12.4 using *Suzaku* X-ray satellite [4] data with high spectral resolution. In addition, spectral simulations of the next-generation satellites, *XRISM* and *Athena* were carried out to see what information could be gleaned from them. In Section 2, observation and data reduction are presented. In Section 3, the analysis and results are given. Section 4 discusses our findings, and Section 5 summarizes future recommendations.

2. X-ray Observation and Data Reduction

In this study, we utilize 19 ks observation data of G278.0+12.4 from *Suzaku* X-ray Imaging Spectrometer [5] on June 24, 2012 (ObsID: 507067010, PI:T.PRINZ). Observation data were taken from CCDs XIS0-3 in 3x3 mode. The data were analyzed using HEASoft software (v.6.32.1), XSPEC (v.12.9.0) [6], and ATOMDB (v.3.0.9) [7, 8]. XSELECT (v.2.5) was used to extract XIS image and spectra from the XIS cleaned event files.

3. Analysis and Results

3.1. Suzaku XIS Image

The image in Fig. 1 shows an XIS1 image of G278.0+12.4 in the range 0.3–10 keV. The DS9

software was utilized to apply logarithmic scaling and coloring to the image.

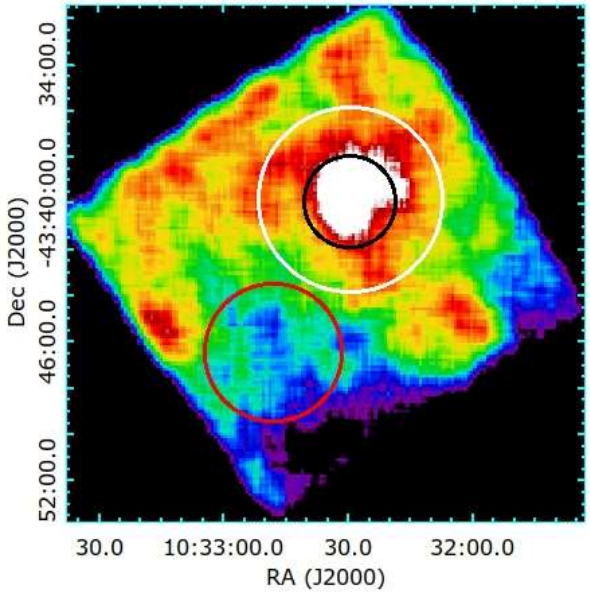

Figure 1. *Suzaku XIS1 image of G278.0+12.4 in the 0.3–10.0 keV energy band. The inner region (radius 2 arcmin) is shown with a black circle and the whole region (radius 4 arcmin) is shown with a white circle. These two regions were extracted separately for spectral analysis. The background region (radius 3 arcmin) is shown with a red circle.*

3.2. *Suzaku* XIS Spectra

We first extracted background spectra in the same FoV but outside G278.0+12.4 (see a red circle in Fig. 1). Since the source is located at high Galactic latitude of b = +12^{O}.4, Galactic Ridge X-ray emission (GRXE) was not considered. We considered non-X-ray background (NXB) and the cosmic X-ray background (CXB) emission. We use fakeit command to simulate the background spectrum. We used this background spectrum in the spectral analysis.

The X-ray spectra of G278.0+12.4 were extracted from two circular elliptical regions. We first used a variable-abundance non-equilibrium ionization (VNEI) model to analyze the spectra. This model also includes the TBabs model [9], which defines the absorption column density (N_H).

To begin the fitting process, the abundance of components was set to solar levels [9]. Despite allowing for freely varying abundances of Ne and Si and those of the other elements are fixed to 1 in units of solar, the fit's decreased □2 remained over 1.5 (inner region : $\chi2$ =1.67 (460 dof) and whole region $\chi2$ =1.61 (1230 dof.)) As a result, the VNEI model was rejected. In XSPEC, we tested vmekal, which is collisional ionization equilibrium plasma model. The outcome was higher $\chi2$ values (whole region: $\chi2$ =1.68 (1220 dof) and inner region: $\chi2$ =1.71 (460 dof). This indicated that rather than fitting a single model, it would be more appropriate to add an extra component to the model. Another plasma model in XSPEC, vmekal, was similarly unsuccessful. We proceeded with the fitting procedure by incorporating a power-law model for non-thermal radiation into the thermal TBabs*(vpshock) model. In the model, N_H, photon index (Γ), and normalization were left free in the power-law model, whereas kTe, □$_u$, and normalization parameters were left free in the vpshock model. All abundances are fixed to the point of solar abundances [9]. Significant results (inner region $\chi2$ = 1.02 (459 dof) and whole region $\chi2$ = 0.99 (1223)) were achieved when one thermal and one non-thermal models were utilized. The derived values' error ranges were not within acceptable bounds when the element abundance values were released during the fit process. Fig. 2 presents the XIS spectra (power-law+1T model). Table 1 displays the best-fit spectral outcomes from the *Suzaku* XIS

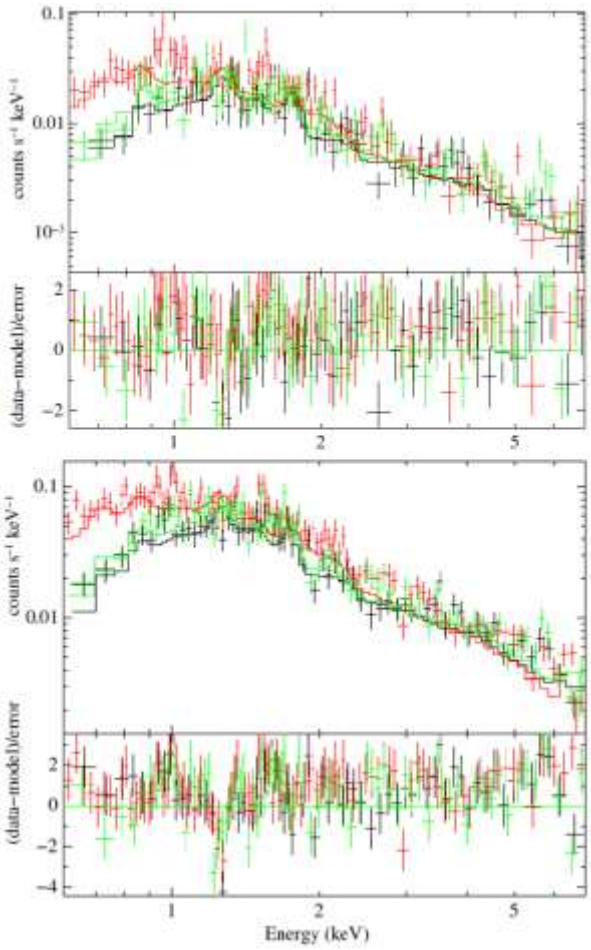

Figure 2. *Suzaku XIS 0, 1 and 3 spectra for the inner (0-2 arcmin) and whole region (0-4 arcmin). Each spectrum has an energy range of 0.6–7.0 keV. The crosshairs in the upper panel show the data, and the solid lines show the applied spectral model. Spectra are overlaid with the best-fitting model.*

Table 1. Best-fitting parameters for G278.0+12.4

Parameters	**Units**	**Model**	**Inner region (0-2 arcmin)**	**Whole region (0-4 arcmin)**
N_H	10^{20} cm^{-2}	TBabs	$5.24^{+0.12}_{-0.13}$	5.22 ± 0.08
kT	keV	Vpshock	$5.33^{+1.56}_{-1.11}$	$4.88^{+0.53}_{-0.63}$
τ_u	10^{10} s cm^{-3}		$4.18^{+0.63}_{-0.65}$	$4.22^{+0.51}_{-0.53}$
Norm[a]	10^{-3} cm^{-5}		62.2 ± 8.97	$58.6^{+1.94}_{-1.93}$
Γ		Power-law	$0.51^{+0.08}_{-0.07}$	$1.01^{+0.18}_{-0.24}$
Norm[b]	10^{-3}		$25.3^{+6.9}_{-5.4}$	15.7 ± 0.02
χ2/dof			1.02 (459)	0.99 (1223)

[a] $Norm = \frac{10^{-14}}{4\pi d^2} \int n_e n_H dV$

where d is the distance to the source (cm), n_e and n_H are the electron and Hydrogen densities (cm^{-3}) respectively.
[b] Photons/keV/cm^2/s at 1 keV.

3.3. *XRISM* and *Athena* spectral simulations

Athena, planned to be launched in 2030s, is the next-generation X-ray telescope. One of *Athena*'s instruments is the revolutionary X-IFU as an X-ray spectrogram [10]. The X-ray Imaging and Spectroscopy Mission (*XRISM*; [11]), launched on 2023 September 7, with the Resolve spectrometer [12]. We performed *XRISM*/Resolve and *Athena*/X-IFU simulations based on *Suzaku* XIS data and model. We used the fakeit command in XSPEC to generate the simulated spectra. Fig. 3 shows the simulated spectra. Each spectrum is simulated for 30 ks in the energy range of 0.6 to 7.0 keV. The emission lines are clearly resolved in both simulated spectra. The abundances of these emission lines allow us to determine the type of SNR.

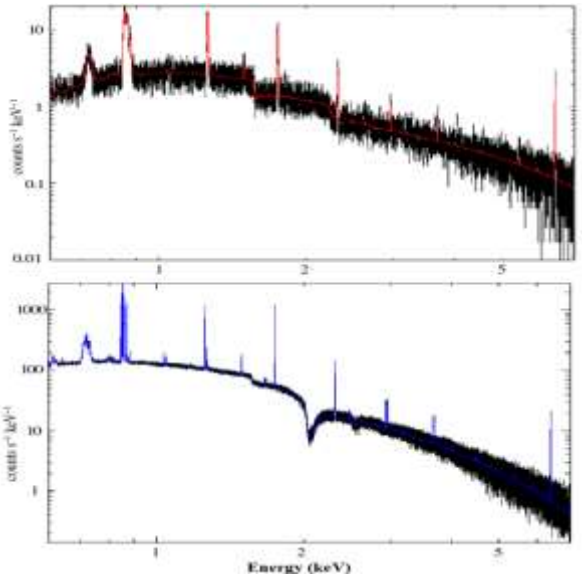

Figure 3. *Simulated spectra of G278+12.4. The top panel represents XRISM/Resolve 30-ks spectra while the bottom panel represents 30-ks Athena/X-IFU spectra. There are the emission lines for Ne, Mg, Si, S, Ar, Ca, and Fe at about 1-1.2 keV, 1.3-1.8 keV, 1.9-2.5 keV, 2.4-3.2 keV, 3.8-5.1 keV, 3.1-4.2 keV, and 6.5 keV, respectively.*

4. Discussion

In this work, we explore the spectral and X-ray characteristics of G278.0+12.4 by *Suzaku*/XIS, which is recognized by the *ROSAT* all-sky Survey

as a potential SNR. Furthermore, spectral simulations of the next-generation satellites, *Athena* and *XRISM*, were carried out.

4.1. X-ray spectral properties of G278.0+12.4

For *Suzaku* data analysis, two regions were selected: the "whole region", which contains all of the emission, and the "inner region", which has the brightest emission. The inner region and whole region were selected with circular areas of radius 0-2 and 0-4 arcmin, respectively. We examined the spectral features for both regions.

We found that the thermal model with a temperature of $5.33^{+1.56}_{-1.11}$ and $4.88^{+0.53}_{-0.63}$ keV for the inner region and the whole region, respectively, and the non-thermal model with a photon index of Γ ~ 0.51 and ~ 1.01 combine to form the spectrum of both regions. As predicted, the inner region kTe value, which is where the emission is most intense, was somewhat higher than the whole region.

Using the normalizing parameter from the vpshock model, we were able to apply to the XIS spectra and estimate the physical characteristics of the X-ray generating plasma (see Table 1). Normalization of the vpshock model,

$$Norm = \frac{10^{-14}}{4\pi d^2} \int n_e n_H dV$$

The formula uses the following values: n_e, n_p, V, and d stand for the electron density (cm^{-3}) (see Table 1). The whole region is a sphere with a radius of 4 arcmin and the volume ($V=4/3\pi R^3$) is the volume of the SNR $V = 1.93 \times 10^{56} f d^3$ cm^3. Here f is the volume filling factor and distance in kpc was used as d. We found an electron density n_e was determined as $0.66 f^{-1/2} d^{-1/2}$ cm^{-3} for fully ionized plasma $n_e=1.2n_H$.

The plasma's ionization timescale is specified by the parameter τ_u (cm^{-3} s):

$$\tau_u = n_e t$$

where t (s) represents the remnant's age and n_e (cm^{-3}) is electron density. Our analysis of electron density and ionization parameters yielded an age of around $2.02 f^{1/2} d^{1/2}$ kyr.

4.2. Future Prospect

The X-ray spectra of G278.0+12.4 obtained from *Suzaku/XIS* data are given in Fig. 2. When comparing the *Suzaku* spectra with the *XRISM/Resolve* and *Athena/X-IFU* simulated spectra, the following differences can be seen: *XRISM/Resolve* and *Athena/X-IFU* detectors have higher energy resolution. Therefore, the number of data points in the simulation is significantly larger than the number of data points in the *Suzaku* spectrum. It will be possible to investigate the detailed relationship of SNR with the *XRISM/Resolve* and *Athena/X-IFU* X-ray satellites with high spectral resolution.

These results indicate that high-resolution data are needed to investigate the origin of radiation from G278.0+12.4 spectra. Our models show that two future missions could resolve the thermal emission lines of weak SNRs and provide a better understanding of the nature of these SNRs.

5. Conclusion

In this work, we have performed the first detailed spectral analysis of G278.0+12.4, using archival *Suzaku* data. We have also obtained *XRISM/Resolve* and *Athena/X-IFU simulations*. We conclude the following:

1. The X-ray spectra of G278.0+12.4 consist of two types of plasmas, one is in a non-equilibrium ionization thermal model, other is a non-thermal model. Using X-ray spectral parameters, we estimated an electron density of $f^{-1/2} d^{-1/2}$ cm^{-3} and an age of G278.0+12.4 as $2.02 f^{1/2} d^{1/2}$ kyr.

2. *Suzaku* spectral analysis suggests that G278.0+12.4 is likely an SNR. The detection of non-thermal X-ray emission in the XIS spectra points to the possibility of a pulsar wind nebula scenario for G278.0+12.4.

3. Our spectral simulations show that upcoming missions will be capable of resolving the thermal emission lines of faint SNRs, offering improved insights into their nature.

Author Statements:

- **Ethical approval:** The conducted research is not related to either human or animal use.
- **Conflict of interest:** The authors declare that they have no known competing financial interests or personal relationships that could have appeared to influence the work reported in this paper
- **Acknowledgement:** The authors declare that they have nobody or no-company to acknowledge.
- **Author contributions:** The authors declare that they have equal right on this paper.

- **Funding information:** The authors declare that there is no funding to be acknowledged.
- **Data availability statement:** The data that support the findings of this study are available on request from the corresponding author. The data are not publicly available due to privacy or ethical restrictions.

References

[1]Trumper, J. (1982). The ROSAT mission. *Advances in Space Researc*h 2: 241–249. DOI: 10.1016/0273-1177(82)90070-9

[2]Vink, J. (2020). Physics and Evolution of Supernova Remnants. *Springer International Publishing*, Cham, Switzerland.

[3]Voges, W., Aschenbach, B., Boller, T., Brauninger, H., Briel, U., Burkert, W. et al. (1999). The ROSAT all-sky survey bright source catalogue. *Astronomy and Astrophysics*. 349: 389-405. DOI: 10.48550/arXiv.astro-ph/9909315

[4]Mitsuda, K., Bautz, M., Inoue, H., Kelley, R.L., Koyama, K., Kunieda, H., et al. (2007), The X-Ray Observatory *Suzaku*. *Publications of the Astronomical Society of Japan.* 59 (1): 1-7. DOI: 10.1093/pasj/59.sp1.S1

[5]Koyama, K., Tsunemi, H., Dotani, T., Bautz, M.W., Hayashida, K., Tsuru, T.G.. et al. (2007). X-Ray Imaging Spectrometer (XIS) on Board *Suzaku*. *Publications of the Astronomical Society of Japan.* 59: 23–33. DOI:10.1093/pasj/59.sp1. S23.

[6]Arnaud, K. A. (1996), XSPEC: The First Ten Years. in Jacoby G. H., Barnes J., eds, ASP Conf. Ser. Vol. 101, *Astronomical Data Analysis Software and Systems V. Astron. Soc. Pac.*, San Francisco, CA, p. 17

[7]Foster, A. R., Ji L., Smith, R.K., Brickhouse, N.S. (2012), Updated Atomic Data and Calculations for X-Ray Spectroscopy. *The Astrophysical Journal*, 756 (1): 128-138. DOI:10.1088/0004-637X/756/2/128

[8]Smith, R.K., Brickhouse, N.S., Liedahl, D.A., Raymond, J.C. (2001). Collisional Plasma Models with APEC/APED: Emission-Line Diagnostics of Hydrogen-like and Helium-like Ions. *The Astrophysical Journal*. 556(2), L91-L95. DOI:10.1086/322992

[9]Wilms, J., Alle, A., McCray, R. (2000), On the Absorption of X-Rays in the Interstellar Medium. *The Astrophysical Journal*. 542 (2), 914-924. DOI: 10.1086/317016

[10]Barret, D., Cucchetti, E. (2018). X-IFU response matrices [online]. Website http://x-ifu-resources.irap.omp.eu/

[11]Tashiro, M., Maejima, H., Toda, K., Kelley, R., Reichenthal, L., Lobell, J. et al. (2018). Concept of the X-ray Astronomy Recovery Mission. *In: Society of Photo-Optical Instrumentation Engineers (SPIE) Conference Series*, 10699, Proc. SPIE, 1069922. DOI:10.1117/12.2309455

[12]Ishisaki, Y., Kelley, R. L., Awaki, H., Balleza, J. C., Barnstable, K. R., Bialas, T.G., et al. (2022). Status of resolve instrument onboard X-Ray Imaging and Spectroscopy Mission (XRISM). *Proceedings of the SPIE*. 12181: 121811S. DOI: 10.1117/12.2630654